

Chemical Composition of *Solanum nigrum* Linn Extract and Induction of Autophagy by Leaf Water Extract and Its Major Flavonoids in AU565 Breast Cancer Cells

HSIU-CHEN HUANG, KAI-YANG SYU, AND JEN-KUN LIN*

Graduate Institute of Biochemistry and Molecular Biology, College of Medicine, National Taiwan University, Taipei, Taiwan

Solanum nigrum Linn (SN) belongs to the Solanaceae family, is a plant growing widely in south Asia, and has been used in traditional folk medicine. It is believed to have antipyretic, diuretic, anticancer, and hepatoprotective effects. During the summertime, this plant has been heavily used to supplement beverages to quench thirst on hot days in Taiwan and several southern Asian countries. In this study, the polyphenols and anthocyanidin in various parts of the SN plant were analyzed by HPLC. The leaves were found to be richer in polyphenols than stem and fruit. SN leaves contained the highest concentration of gentisic acid, luteolin, apigenin, kaempferol, and *m*-coumaric acid. However, the anthocyanidin existed only in the purple fruits. Additionally, the cytotoxicity of the leaf, stem, or fruit extract was evaluated against cancer cell lines and normal cells. The results showed that AU565 breast cancer cells were more sensitive to the extract. Furthermore, the results demonstrated a significant cytotoxic effect of SN leaf extract on AU565 cells that was mediated via two different mechanisms depending on the exposure concentrations. A low dose of SN leaf extract induced autophagy but not apoptosis. Higher doses (>100 $\mu\text{g/mL}$) of SN leaf extract could inhibit the level of p-Akt and cause cell death due to the induction of autophagy and apoptosis. However, these findings indicate that SN leaf extract induced cell death in breast cells via two distinct antineoplastic activities, the abilities to induce apoptosis and autophagy, therefore suggesting that it may provide a useful remedy to treat breast cancer.

KEYWORDS: *Solanum nigrum* Linn; autophagy; polyphenols; anthocyanidin; AU565

INTRODUCTION

Solanum nigrum Linn (SN) (**Figure 1**) is an herbal plant that commonly grows in the pen fields of temperate climate zones of Asia. It has been used in traditional folk medicine and is believed to have various biological activities. For example, Chinese people use it to cure inflammation (1) and edema by its antipyretic and diuretic effects. It is used as a hepatoprotective agent (2, 3) and for treating various kinds of tumors (4), including liver cancer, breast cancer, lung cancer, stomach cancer, colon cancer, and bladder cancer. The water extracts of SN (SNE) suppressed oxidant-mediated DNA-sugar damage (5), exerted cytoprotection against gentamicin-induced toxicity on Vero cells (6), induced necrosis in SC-M1 stomach cancer cells (7), and inhibited 12-*O*-tetradecanoylphorbol-13-acetate-induced tumor promotion in MCF-7 cells (8) and antineoplastic activity against Sarcoma 180 in mice. It has also been demonstrated that an ethanol extract from fruits of SN had a remarkable hepatoprotective effect in CCl₄-induced liver damage (3), inhibited the proliferation of human MCF-7

breast cancer cells, and induced cell death by apoptosis (9). Recently, Wang et al. reported that SNE suppressed AAF-induced hepatic injury and early hepatocarcinogenesis through overexpression of glutathione *S*-transferases, Nrf2, and antioxidant enzymes (10). These studies suggest that SN possesses a beneficial activity as an antioxidant and antitumor-promoting agent, although the mechanism for the activity remains to be elucidated.

The whole plant of *S. nigrum* has also been detected to contain many steroidal glycosides, steroidal alkaloids, and steroidal oligoglycosides (4, 11), including solamargine, solasonine, solavil-line, solasdamine, and solanine. The activities of such alkaloids could be used for antitumor purposes (12). Besides, it has been reported to contain many polyphenolic compounds (9, 13), including gallic acid, protocatechuic acid, catechin, caffeic acid, epicatechin, rutin, and naringenin; the antioxidant and antitumor activities may be due to the presence of polyphenolic constituents. Furthermore, a 150 kDa glycoprotein isolated from *S. nigrum* Linn has been reported and could reduce inducible nitric oxide (iNO) production and has an apoptotic effect in HCT-116 cells (14)

Autophagy, or “self-eating”, is an evolutionarily conserved catabolic process by which cytoplasmic contents and organelles (including long-lived proteins and damaged organelles) are > delivered to the lysosome, where degradative enzymes break the

*Address correspondence to this author at the Institute of Biochemistry and Molecular Biology, College of Medicine, National Taiwan University, No. 1, Section 1, Jen-ai Road Taipei, Taiwan [telephone (886)-2-2356-2213; fax (886)-2-2391-8944; e-mail jklin@ha.mc.ntu.edu.tw].

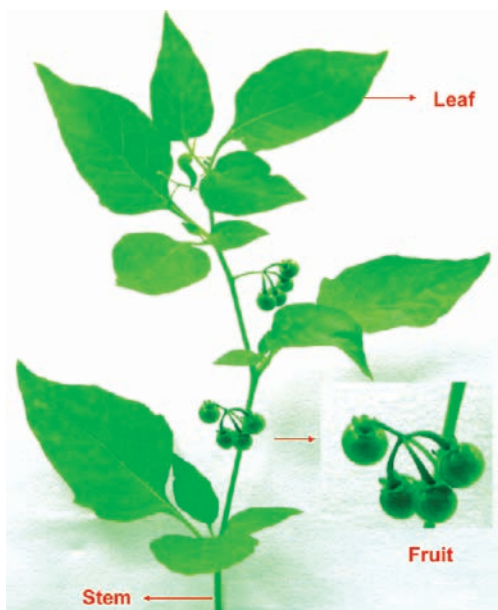


Figure 1. *Solanum nigrum* Linn (SN). The picture was taken in the College of Law and Social Sciences, National Taiwan University, Taipei, Taiwan. The fruit is a green berry, 6–8 mm in diameter, that turns purple-black when ripe.

vesicle down (15)). Autophagy has a fundamental role in normal organisms, allowing them to adapt to and survive despite stress (16). Recently it has further been found that autophagy may be a transitory tactical response and has a greater variety of physiological and pathophysiological roles (17) than expected, such as starvation, adaptation, development, intracellular protein degradation, organelle clearance, antiaging, elimination of microorganisms (18), cell death, tumor suppression, and antigen presentation. Moreover, there is a potential link between autophagy and a number of diseases in humans. For instance, cancer, neurodegenerative disorders such as Alzheimer's, Parkinson's, and Huntington's diseases (19), cardiomyopathy, amyotrophic lateral sclerosis, and prion diseases are all associated with increased autophagy activity. However, the precise role that autophagy plays in cancer development, disease progression, tumor maintenance, and the response to anticancer therapies is very controversial. Indeed, several agents such as arsenic trioxide (20), rapamycin (21), and tamoxifen (22, 23) are believed to induce autophagic cell death in certain cell types. However, autophagy can also provide protection from cell death in times of stress. Therefore, the impact of autophagy induction on the efficacy of chemotherapeutic drugs can be highly variable and cell type and treatment dependent. Despite this dichotomy, in certain settings the induction of autophagy is likely to be of therapeutic benefit.

Although SN has been reported to have antifungal, antitumor, anti-inflammation, antioxidative, anticarcinogenesis, and antimutagenesis abilities, practically nothing is known of the pharmacological effects of this plant. Furthermore, whether the leaves, stems, or fruits of SN are poisonous or not is being intensively discussed, and it is believed that the toxic effects vary considerably according to the part of the plant being used. Therefore, the purpose of this work was to evaluate whether the extracts of SN exert the claimed antitumor actions, and extracts of different parts of SN, such as leaf, stem, immature fruit, and mature fruit, were prepared and used in the assays.

MATERIALS AND METHODS

Preparation of the Water Extracts of *Solanum nigrum* (SNE). One hundred grams of dried different parts of SN (leaf, stem, green fruit,

or purple fruit) was immersed in 2000 mL of distilled water for 30 min and then boiled at 95 °C for 30 min. After cooling, the extracts were filtered by a paper filter. The SNE were obtained after evaporation of water to dryness in a vacuum rotary evaporator at 80 °C that finally gave 28.75 g (28.75% of initial amount) of powder (SNE). The concentration used in the experiment was based on the dry weight of the extract.

Determination of Total Polyphenol Content. The total polyphenol content was determined by spectrophotometry, using gallic acid as standard, according to the Folin–Ciocalteu method. Briefly, 1.0 mL of the diluted sample extract was transferred in duplicate to separate tubes containing 5.0 mL of a 1/10 dilution of Folin–Ciocalteu's reagent in water. Then, 3.0 mL of a 2% Na₂CO₃ solution was added. Absorbance of the mixture was measured at 750 nm.

Reverse-Phase HPLC Analysis of SNE. The determination of polyphenols and anthocyanins was carried out by high-performance liquid chromatography (HPLC). For polyphenol composition analysis, water extract (1 g, dried powder) of SN was extracted three times with 50 mL of ethyl acetate to obtain an ethyl acetate-soluble part (0.198 g). The HPLC used a 250 × 4.6 mm i.d., 5 μm Thermo 5 C18-MS packed column (Nacalai Tesque, Inc., Kyoto, Japan). Briefly, gradient elution was employed with a mobile phase consisting of 40% acetonitrile (solution A) and 5% acetonitrile (solution B) as indicated in Figure 2A-1,A-2. The flow rate was 1 mL/min. The column was maintained at 30 °C. The polyphenols were detected by UV at 295 nm.

For determination of anthocyanins, 10 g of dried different parts of SNE was extracted with 30 mL of 2 N HCl (in methanol/distilled water = 1:1) for 1 h. The supernatant was then collected and boiled at 95 °C for 0.5, 1, 2, and 3 h, respectively. The HPLC used a 250 × 4.6 mm i.d., 5 μm Cosmosil 5 C18-MS packed column (Nacalai Tesque, Inc.). Briefly, the mobile phase was acetonitrile/distilled water/trifluoroacetic acid (195:805:4 v/v/v), and the flow rate was 1 mL/min. The column was maintained at 30 °C. The anthocyanidins were detected by UV at 530 nm as indicated in Figure 2B-1,B-2.

Cell Lines and Cell Cultures. Human breast cancer lines, such as AU565, which overexpresses Her-2, MCF-7, which expresses the basal level of Her-2, and HBL-100, which is derived from normal human breast tissue transformed by SV40 large T antigen and expresses a basal level of Her-2, were used in this study. All breast cancer cell lines and Hep-G2 and NIH-3T3 were purchased from ATCC and cultured in DMEM supplemented with 10% fetal calf serum and 1% penicillin–streptomycin. These cells were grown at 37 °C in a humidified atmosphere of 5% CO₂.

Cell Viability Assays. The effect of SN water extracts on cell viability was examined by MTT assay. Briefly, cells were seeded in a 24-well flat-bottom plate overnight. Cells were then treated with various concentrations of SNE or polyphenols. After incubation for various times, 300 μL of MTT solution (0.5 mg/mL, Sigma Chemical Co.) was added to each well and incubated for 4 h at 37 °C. The supernatant was aspirated, and the MTT–formazan crystals formed by metabolically viable cells were dissolved in DMSO. Finally, the absorbance was monitored by a microplate reader at a wavelength of 550 nm.

Cell Proliferation Assay by Cell Counting. The trypan blue dye exclusion assay was used to determine the cytotoxic effect of SN leaf on cells. Briefly, cells were seeded on 6-well dishes overnight and then incubated with different concentrations of SN leaf for various times. At the end of the incubation periods, the cells were harvested by trypsinization. The cells were mixed well with trypan blue solution, and the live cells without dye staining inside were counted by a hemocytometer under a microscope.

Western Blot Analyses and Antibodies. Cells were harvested and homogenized by using Golden lysis buffer (10% glycerol, 1% Triton X-100, 1 mM sodium orthovanadate, 1 mM EGTA, 5 mM EDTA, 10 mM NaF, 1 mM sodium pyrophosphate, 20 mM Tris-HCl, pH 7.9, 100 μM β-glycerophosphate, 137 mM NaCl, 1 mM PMSF, 10 μg/mL aprotinin, and 10 μg/mL leupeptin) for 30 min at 4 °C. Protein content was determined against a standardized control, using the Bio-Rad protein assay kit (Bio-Rad Laboratories). The protein inputs in the Western blot analyses were normalized by loading equal amounts of total protein lysates into the SDS-PAGE gel, transferred onto polyvinylidene difluoride membranes, and then probed with primary antibody followed by secondary antibody conjugated with horseradish peroxidase. Reactive bands were visualized with an enhanced chemiluminescence system (Amersham Biosciences, Arlington Heights, IL). The intensity of the bands was scanned and

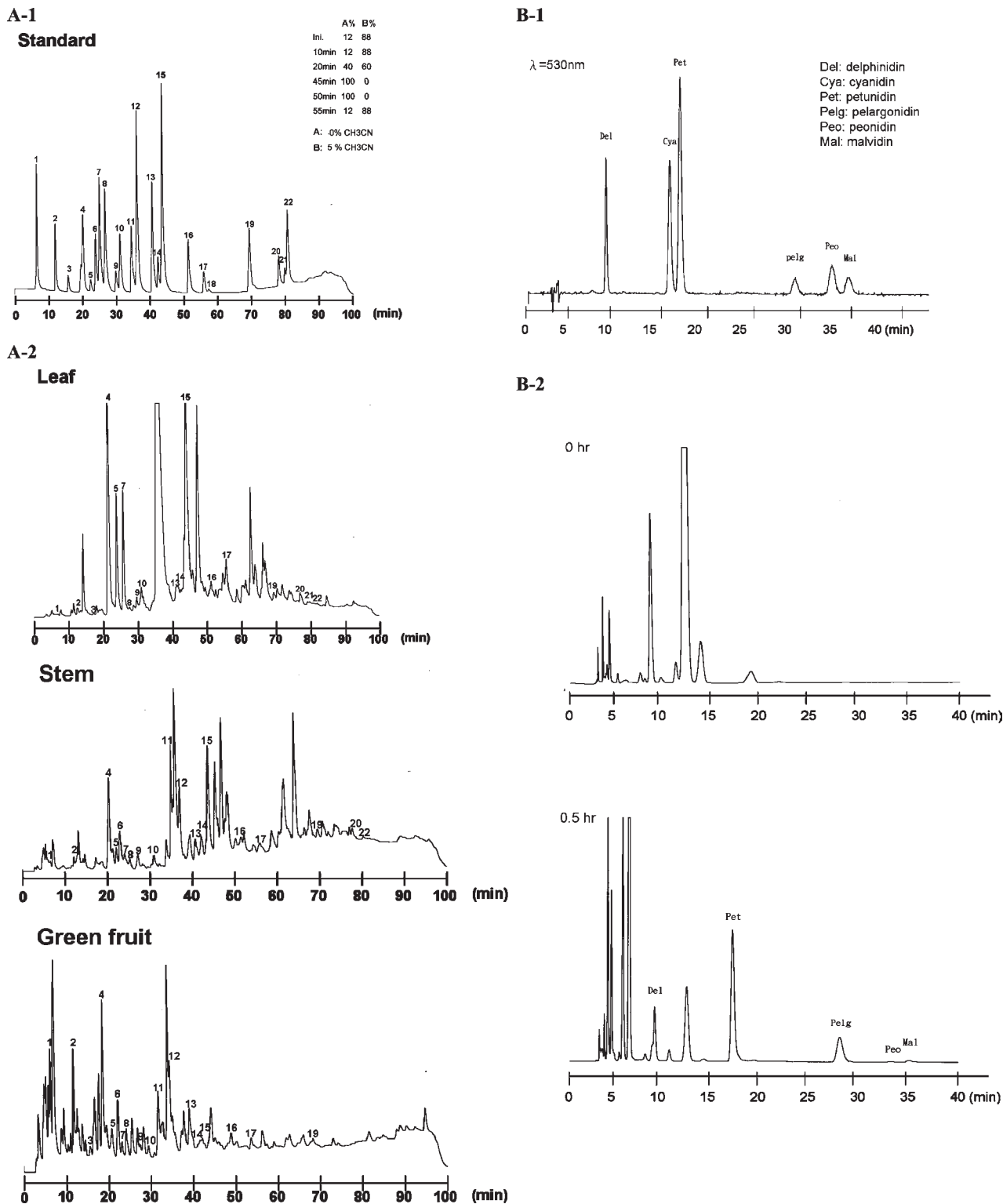


Figure 2. Analysis of polyphenol and anthocyanidin content in SN extract. **(A-1)** HPLC chromatograms of the polyphenol standard mixture recorded at 295 nm. The HPLC used a 250×4.6 mm i.d., $5 \mu\text{m}$ Thermo 5 C18-MS packed column (Nacalai Tesque, Inc.). Briefly, gradient elution was employed with a mobile phase consisting of 40% acetonitrile (solution A) and 5% acetonitrile (solution B) as indicated in the figure. Polyphenol compounds corresponding to peaks in part **A-2** are marked. **(A-2)** Polyphenols in SN extract were analyzed by HPLC. Peaks: 1, gallic acid; 2, protocatechuic acid; 3, epigallocatechin (EGC); 4, chlorogenic acid + catechin; 5, gentisic acid; 6, vanillic acid; 7, caffeic acid; 8, syringic acid; 9, epicatechin (EC); 10, epigallocatechin gallate (EGCG); 11, galocatechin gallate (GCG); 12, *p*-coumaric acid; 13, ferulic acid; 14, rutin; 15, *m*-coumaric acid; 16, narigenin; 17, luteolin; 18, myricetin; 19, quercetin; 20, apigenin; 21, kaempferol; 22, hesperetin. **(B-1)** HPLC chromatograms of the anthocyanin standard mixture recorded at 530 nm. The HPLC used a 250×4.6 mm i.d., $5 \mu\text{m}$ Cosmosil 5 C18-MS packed column (Nacalai Tesque, Inc.). The mobile phase was acetonitrile/distilled water/trifluoroacetic acid (195:805:4 v/v/v), and the flow rate was 1 mL/min. Abbreviations: Del, delphinidin; Cya, cyanidin; Pet, petunidin; Pelg, pelargonidin; Peo, peonidin; Mal, malvidin. **(B-2)** After acid hydrolysis, we can detect Del, Pet, Pelg, Peo, and Mal in purple fruit of *S. nigrum* but not in green fruit.

quantified with National Institute of Health image software. Antibodies against Akt, phospho-Akt (Ser473), AMPK, phospho-AMPK (Thr172), and c-PARP were purchased from Cell Signaling Technology (Beverly, MA); antibodies against LC-3 and phospho-mTOR and anti- β -actin antibody were purchased from Sigma Chemical Co. (St. Louis, MO). Anti-mouse and anti-rabbit antibodies conjugated to horseradish peroxidase were obtained from Santa Cruz Biotechnology (Santa Cruz, CA).

ATP Level Determination. The ATP level was determined with regard to the protocol of an ATP lighting kit. Cells were incubated in a 96-well flat-bottom plate overnight. Cells were incubated with an ATPase light kit after SNE had been treated for various times. The cells were lysed with lysis buffer, and transferred to a light-avoiding black 96-well dish, and the luminescence was measured by an ELISA reader.

Flow Cytometric Analysis of Apoptosis, Cell Cycle. For the flow cytometric analysis, cells were seeded on 60 mm Petri dishes overnight and then incubated with different concentrations of SNE for various times. For the analysis of cell cycle and apoptosis, cells were stained with propidium iodide (PI). After SNE treatment, cells were trypsinized and washed twice with ice-cold phosphate-buffered saline (PBS), and the cells were fixed with 70% ice-cold ethanol overnight at -20°C . Following 1500 rpm centrifugation, the cell pellets were treated by RNase A, stained with PI, and then analyzed by flow cytometry (FACScan, BD Biosciences, Mountain View, CA). The percentage of sub-G1 fraction was analyzed by using Cell Quest software (BD Biosciences).

Microscope Observation of Cellular Morphology, Autophagic Vascular Organelle (AVO), Nuclear Morphology. For microscope observation, cells were cultured overnight in 6-well dishes with glass slides inside and then incubated with different concentrations of SNE for various times. After SNE treatment, the cellular morphology was observed directly by light microscope. To observe the autophagic vascular organelle (AVO), cells were stained with serum-free medium containing $10\ \mu\text{g}/\text{mL}$ of mono-

dansyl dacarbencine (MDC). After 30 min of incubation, cells were washed with PBS and fixed with 4% formaldehyde for 30 min. After fixation, cells were washed with PBS and observed by fluorescence microscope. For nuclear morphology observation, cells were fixed with 4% formaldehyde for 30 min, washed with PBS, then incubated with $\mu\text{g}/\text{mL}$ DAPI for 30 min, washed with PBS three times, and observed by fluorescence microscope.

Statistical Analysis. All values were expressed as mean \pm SD. Each value is the mean of at least three separate experiments in each group. Student's *t* test was used for statistical comparison. Asterisks (*) indicate the values are significantly different from the control: *, $p < 0.05$; **, $p < 0.01$; ***, $p < 0.001$.

RESULTS

Chemical Composition of SNE. To establish the composition of SNE from SN, the contents of polyphenols and anthocyanins

Table 1. Contents (Micrograms per Gram) of Phenolic Acids in Different Parts of SN

peak	retention time (min)	leaf	stem	green fruit
1	6.70	0.53 \pm 0.5	1.36 \pm 0.77	29.33 \pm 2.27
2	11.85	10.59 \pm 4.59	6.15 \pm 4.09	56.50 \pm 4.93
3	14.99	16.92 \pm 5.01	nd	281.46 \pm 7.06
5	20.99	2489.00 \pm 212.86	249.70 \pm 95.24	437.58 \pm 118.23
6	22.18	nd	20.62 \pm 7.56	40.36 \pm 5.92
7	23.12	82.24 \pm 9.87	7.89 \pm 5.12	11.78 \pm 4.63
8	24.58	9.42 \pm 7.04	5.07 \pm 2.28	13.70 \pm 3.94
9	27.89	65.70 \pm 12.23	26.17 \pm 8.41	51.56 \pm 25.78
10	29.27	30.38 \pm 11.93	8.96 \pm 0.38	19.20 \pm 4.11
11	32.73	19.58 \pm 9.18	44.02 \pm 10.09	30.51 \pm 15.48
12	34.69	7.85 \pm 5.84	19.82 \pm 5.75	34.78 \pm 21.97
13	39.08	15.86 \pm 7.19	15.89 \pm 5.39	33.41 \pm 7.39
14	40.48	41.65 \pm 9.10	49.45 \pm 6.45	9.45 \pm 5.90
15	41.69	183.40 \pm 14.91	26.44 \pm 6.72	8.41 \pm 5.69
16	48.75	26.20 \pm 8.05	7.93 \pm 5.58	8.80 \pm 5.92
17	53.38	1091.33 \pm 315.38	198.93 \pm 70.33	210.32 \pm 80.34
18	54.99	nd	nd	nd
19	67.52	14.85 \pm 5.89	10.75 \pm 5.70	10.94 \pm 5.92
20	76.39	354.06 \pm 93.45	106.32 \pm 77.03	nd
21	78.25	315.65 \pm 375.55	nd	nd
22	79.04	142.75 \pm 116.54	125.86 \pm 113.03	nd

Table 2. Contents (Micrograms per Gram) of Anthocyanidins in Purple Fruits of SN after Acid Hydrolysis at 95°C for 0.5, 1, 2, and 3 h, Respectively

UV λ_{max} (nm)	540	531	536	511	528	537	
retention time (min)	8.5	15.3	16.4	28.7	32.8	34.7	
hydrolysis time (h)	Del	Cya	Pet	Pelg	Peo	Mal	total
0	nd	nd	nd	nd	nd	nd	nd
0.5	144.87 \pm 25.28	nd	174.64 \pm 59.81	867.38 \pm 67.67	29.87 \pm 20.37	64.49 \pm 22.00	1281.23
1	202.73 \pm 28.41	nd	306.17 \pm 76.95	57.96 \pm 36.20	23.02 \pm 20.33	117.8 \pm 21.13	707.67
2	106.98 \pm 18.44	nd	188.98 \pm 58.39	nd	nd	66.95 \pm 24.75	362.91
3	49.13 \pm 16.55	nd	102.59 \pm 53.60	nd	nd	33.54 \pm 21.13	185.27

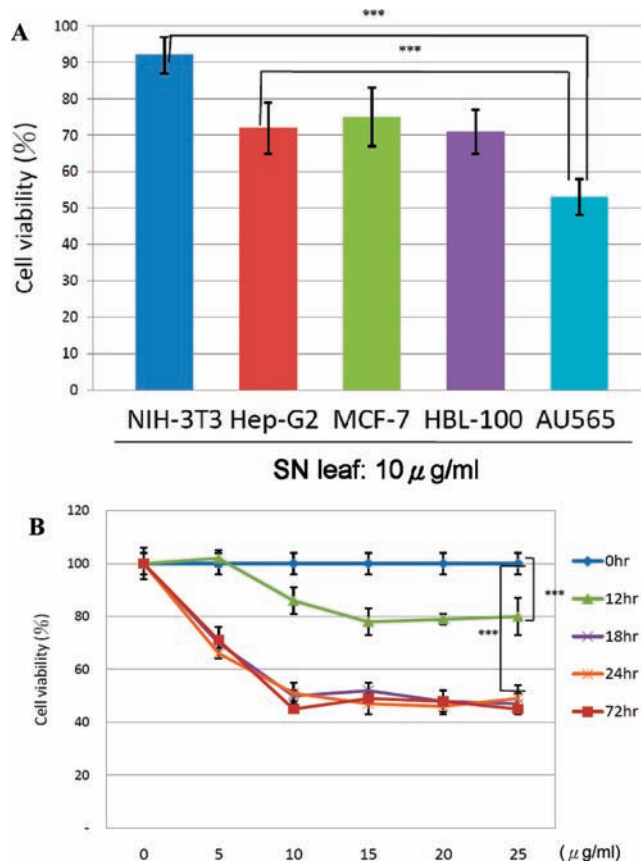


Figure 3. Cell viability comparison of different cell lines treated by SN leaf. (A) MTT assay showed the different responses of cell lines treated by $10\ \mu\text{g}/\text{mL}$ SN leaf for 24 h. AU565 was more sensitive to SN leaf treatment than HBL-100, MCF-7, Hep-G2, and NIH-3T3. All values are expressed as mean \pm SD. Asterisks (*) indicate the values are significantly different from the control: *, $p < 0.05$; **, $p < 0.01$; ***, $p < 0.001$, $n \geq 3$. (B) Cell viability of AU565 cells with various concentrations of SN leaf at indicated times. Cell viability curve was determined by MTT assay and analyzed.

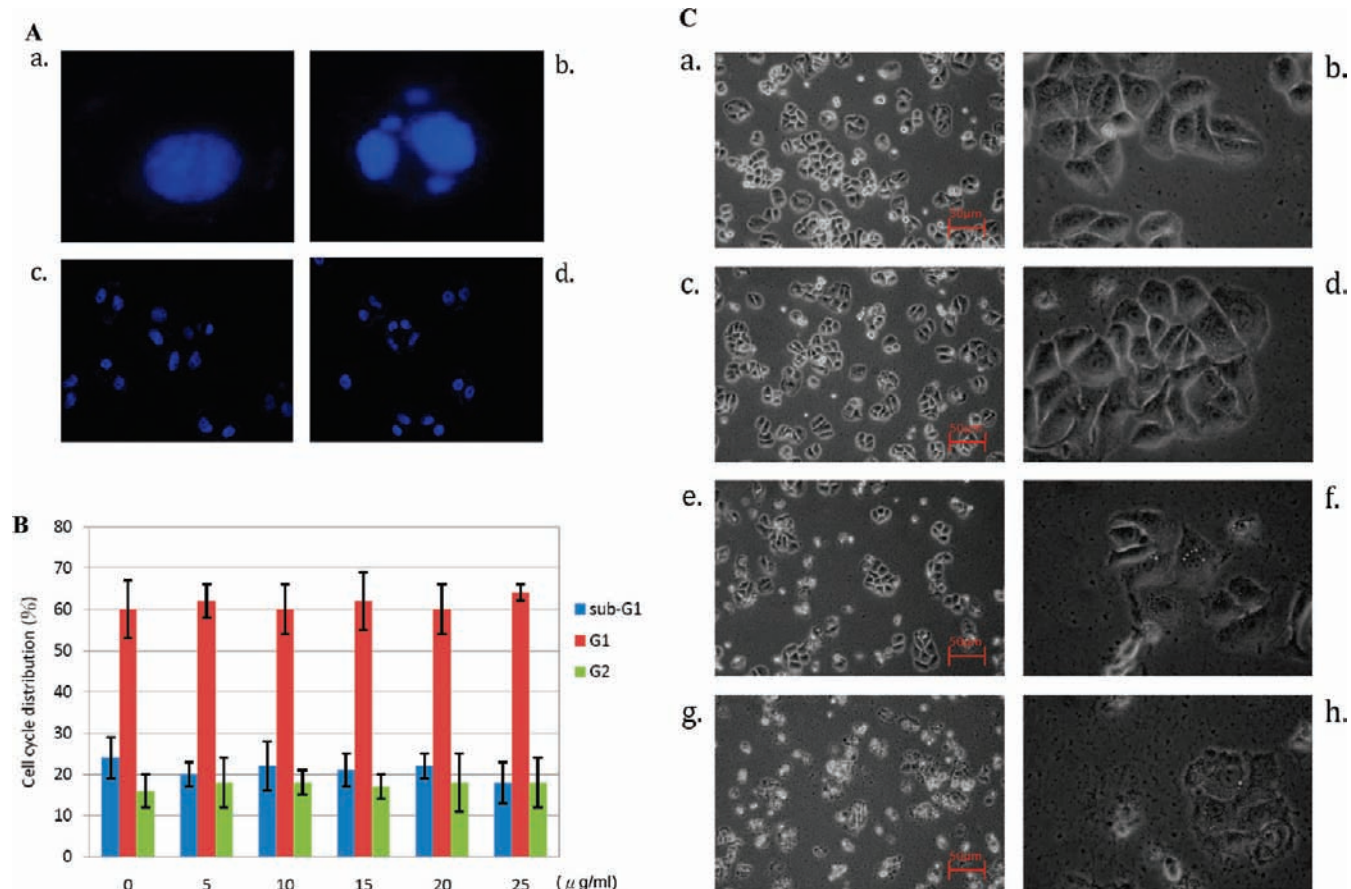


Figure 4. SN leaf treatment below 25 $\mu\text{g/mL}$ would not induce apoptosis, analyzed by DAPI staining and flow cytometer. **(A)** Nucleus of AU565 was stained by DAPI and observed by fluorescence microscope: (a) normal nucleus; (b) DNA fragmentation of apoptotic nucleus; (c, d) nuclear observation of AU565 treated by 0 and 25 $\mu\text{g/mL}$ SN leaf for 48 h (400 \times original magnification). **(B)** Cell cycle distribution was assessed by flow cytometry. All values were expressed as mean \pm SD (* indicates the values are significantly different from the control (*, $p < 0.05$; **, $p < 0.01$; ***, $p < 0.001$), $n \geq 3$). **(C)** Morphological changes of AU565 cells were induced by SN leaf for 72 h. AU565 cells were treated with different concentrations of SN leaf for 72 h. The morphological changes in AU565 cells were noted by light microscopic observation. (100 \times or 1000 \times original magnification): (a, b) 0 $\mu\text{g/mL}$; (c, d) 25 $\mu\text{g/mL}$; (e, f) 50 $\mu\text{g/mL}$; (g, h) 100 $\mu\text{g/mL}$ (a, c, e, and g were 100 \times original magnification; b, d, f, and h were 1000 \times original magnification).

were assayed, and the concentrations of polyphenols and anthocyanins were determined by HPLC. The dry weight yield of SNE was $28.75 \pm 4.15\%$, consisting of $22.15 \pm 1.41\%$ total polyphenolics using gallic acid as the standard (data not shown). For polyphenol composition analysis, the SNE was partitioned by ethyl acetate three times, and then water was evaporated to dryness in a vacuum rotary evaporator at 45 $^{\circ}\text{C}$. In Figure 2A-1, HPLC analysis showed the standard of polyphenols, including 13 flavonoids [epigallocatechin (EGC), epicatechin (EC), epigallocatechin gallate (EGCG), galocatechin gallate (GCG), catechin, rutin, narigenin, luteolin, myricetin, quercetin, apigenin, kaempferol, hesperetin] and 10 phenolic acids (gallic acid, protocatechuic acid, chlorogenic acid, gentisic acid, vanillic acid, caffeic acid, syringic acid, *p*-coumaric acid, ferulic acid, *m*-coumaric acid). The contents of these polyphenols in the leaf, stem, and green fruit extracts of SN were analyzed and are summarized in Figure 2A-2 and Table 1. The results indicate gentisic acid is the most abundant as compared to other polyphenols in every part of SN; luteolin is second.

As shown in Figure 2B-1, HPLC analysis of the standard anthocyanidin showed that the retention times of delphinidin, cyanidin, petunidin, pelargonidin, peonidin, and malvidin were 8.5, 15.3, 16.4, 28.7, 32.8, and 34.7 min, respectively. By use of acid hydrolysis, we could detect anthocyanidin (the acid hydrolysis product anthocyanin) in the extracts of purple fruits. Before acid hydrolysis, no anthocyanidin was detected in the purple

fruits (data not shown). After acid hydrolysis, however, the hydrolysis product of anthocyanin was analyzed and is summarized in Figure 2B-2 and Table 2. The analysis of SNE from purple fruits revealed the concentrations of delphinidin, petunidin, pelargonidin, peonidin, and malvidin were 202.73 ± 28.41 , 306.17 ± 76.95 , 867.38 ± 67.67 , 29.87 ± 20.37 , and $117.8 \pm 21.13 \mu\text{g/g}$, respectively. Under similar conditions, we could not detect the presence of the above-mentioned anthocyanidin or its hydrolyzed product anthocyanin in the extracts of leaves, stems, and green fruits of SN (data not shown). Taken together, our results suggest that the anthocyanin existed only in the purple fruits of SN.

AU565 Was More Sensitive to the Water Extract of *Solanum nigrum* Linn Leaf. In this study, we first made the water extracts of SN leaf, stem, or fruit for comparison of their cytotoxic effects. Comparison of the toxicity to liver cancer (Hep-G2 cells), breast cancer (MCF-7 and AU565 cells), and relative normal cells (NIH-3T3 and HBL-100 cells) showed that SN raw fruit exhibited more toxicity to NIH-3T3 (data not shown). SN stem exhibited more toxicity to immortalized HBL-100 breast epithelial cells (data not shown). SN leaf extracts exhibited relatively low toxicity to NIH-3T3, whereas AU565 breast cancer cells showed the most sensitivity to SN leaf extract unexpectedly (Figure 3A). Here, we tested how SN leaf affected AU565. After 10 $\mu\text{g/mL}$ treatment for 24 h, the cell viability of AU565 decreased to about 55%. In comparison with other cell lines, this cell line was most sensitive to the

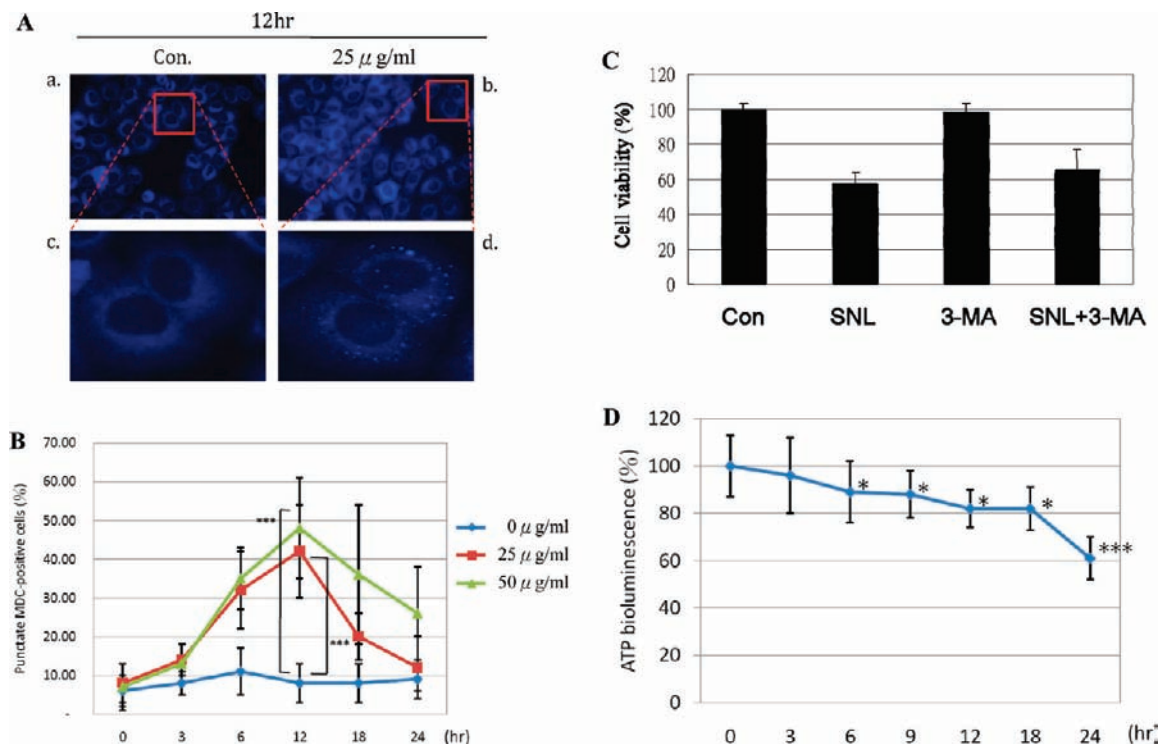


Figure 5. SN leaf treatment induced autophagic vascular organelle (AVO) formation between 6 and 18 h. (A) After treatment with various concentrations of SN leaf for different times, cells were stained with MDC. The punctuated MDC positive cells increased after 6 h and decreased after 18 h of treatment. (a, c) 0 $\mu\text{g/mL}$ as control; (b, d) 25 $\mu\text{g/mL}$; (a, b) 400 \times original magnification; (c) field enlarged from a; (d) field enlarged from b. (B) Quantification of MDC-positive cells after 0, 25, and 100 $\mu\text{g/mL}$ SN leaf treatment. $n \geq 3$. (C) 3-MA decreases SN leaf-induced cell death. Cells were exposed to DMSO, 10 $\mu\text{g/mL}$ SN leaf, or cotreatment with 3-MA (1 mM) for 24 h. Cell viability was analyzed by MTT assay. (D) ATP level reduced in AU565 after SN leaf treatment. AU565 was treated with 25 $\mu\text{g/mL}$ SN leaf. The ATP level decreased slowly to about 80% before 18 h. At 24 h, the ATP content was down to about 60%. The percentage was compared to DMSO-treated control. All values are expressed as mean \pm SD (* indicates the values are significantly different from the control: *, $p < 0.05$; **, $p < 0.01$; ***, $p < 0.001$), $n \geq 3$.

water extract of SN leaf. This suggested that SN leaf may have chemotherapeutic potential in AU565 breast cancer, and for such reason we chose AU565 for further studies to determine if the cytotoxic effect of SN leaf in AU565 was dose and time dependent. Various doses of SN leaf (0, 5, 10, 15, 20, 25, 50, 100 $\mu\text{g/mL}$) were used for different time lengths (6, 12, 18, 24, 48, 72 h), and the cell viability was analyzed by MTT assay as shown in Figure 3B. The decrease of cell viability started at the dose of 5 $\mu\text{g/mL}$ and at the time of 12 h. When treated with 10 $\mu\text{g/mL}$ SN leaf, the cell viability decreased to about 50% at the time of 18 h. However, no more toxic effect was observed after treatment for longer times (18–72 h) or with higher doses (10–25 $\mu\text{g/mL}$).

SN Leaf Did Not Induce AU565 Cells into Cycle Arrest or Apoptosis below 25 $\mu\text{g/mL}$. To identify whether SN leaf induced AU565 into cycle arrest or apoptotic cell death, first, DAPI was used to stain the nucleus; nuclear morphology was observed because apoptosis could be characterized by DNA fragmentation and chromatin condensation. Compared with the control group, Figure 4A showed no significant difference in the nuclear morphology observation in the SN leaf treated group.

Second, as shown in Figure 4B, the sub-G1, G1, or G2 phase observed by PI staining and flow cytometer was not significantly different between control and SN leaf treated groups. Third, Figure 4C shows no more apoptotic bodies were observed when compared with control group. Fourth, as our data show in Figure 6, the apoptosis-related protein, c-PARP, did not change. These results indicate that below 25 $\mu\text{g/mL}$ SN leaf treatment did not induce a typical apoptosis in AU565 cells. These observations indicate that no apoptotic effect was initiated in AU565 cells in response to the SN leaf treatment below 25 $\mu\text{g/mL}$.

SN Leaf-Induced Autophagic Cell Death in AU565 Cells. Non-apoptotic programmed cell death is principally attributed to autophagy (type II programmed cell death). Autophagy is a series of biochemical steps through which eukaryotic cells commit suicide by degrading their own cytoplasm and organelles through a process in which these components are engulfed and then digested in double membrane bound vacuoles called autophagosomes (15). To determine whether the SN leaf treatment will induce autophagy, cells were stained with MDC to detect AVO formation. Figure 5A shows the punctuated MDC positive cells at 25 $\mu\text{g/mL}$ SN leaf treatment as compared to control. Figure 5B shows that after treatment with 25 and 100 $\mu\text{g/mL}$ SN leaf, AVO formation increased to about 42 and 45% at the time of 12 h with a great variation in independent experiments. The AVO positive cells decreased after 18 h of treatment. To confirm the contribution of autophagy in the SN leaf-induced cell death, we used the autophagy inhibitor 3-MA, a class III-PI3K inhibitor, to inhibit the autophagy. The MTT assays show that 1 mM 3-MA could partially prevent SN leaf-induced cell death (Figure 5C). On the basis of these data, we concluded that SN leaf could induce AU565 cells to undergo autophagic cell death.

Effect of SN Leaf on the Intracellular ATP Concentration. Autophagic sequestration has previously been shown to correlate positively with intracellular ATP levels (24), suggesting a requirement for energy. To check whether SN leaf might induce autophagy by altering the intracellular ATP concentration, we measured the ATP level with an ATPase lighting kit. As shown in Figure 5D, the ATP content slowly reduced to about 60% when compared to control. This result suggested that SN leaf treatment

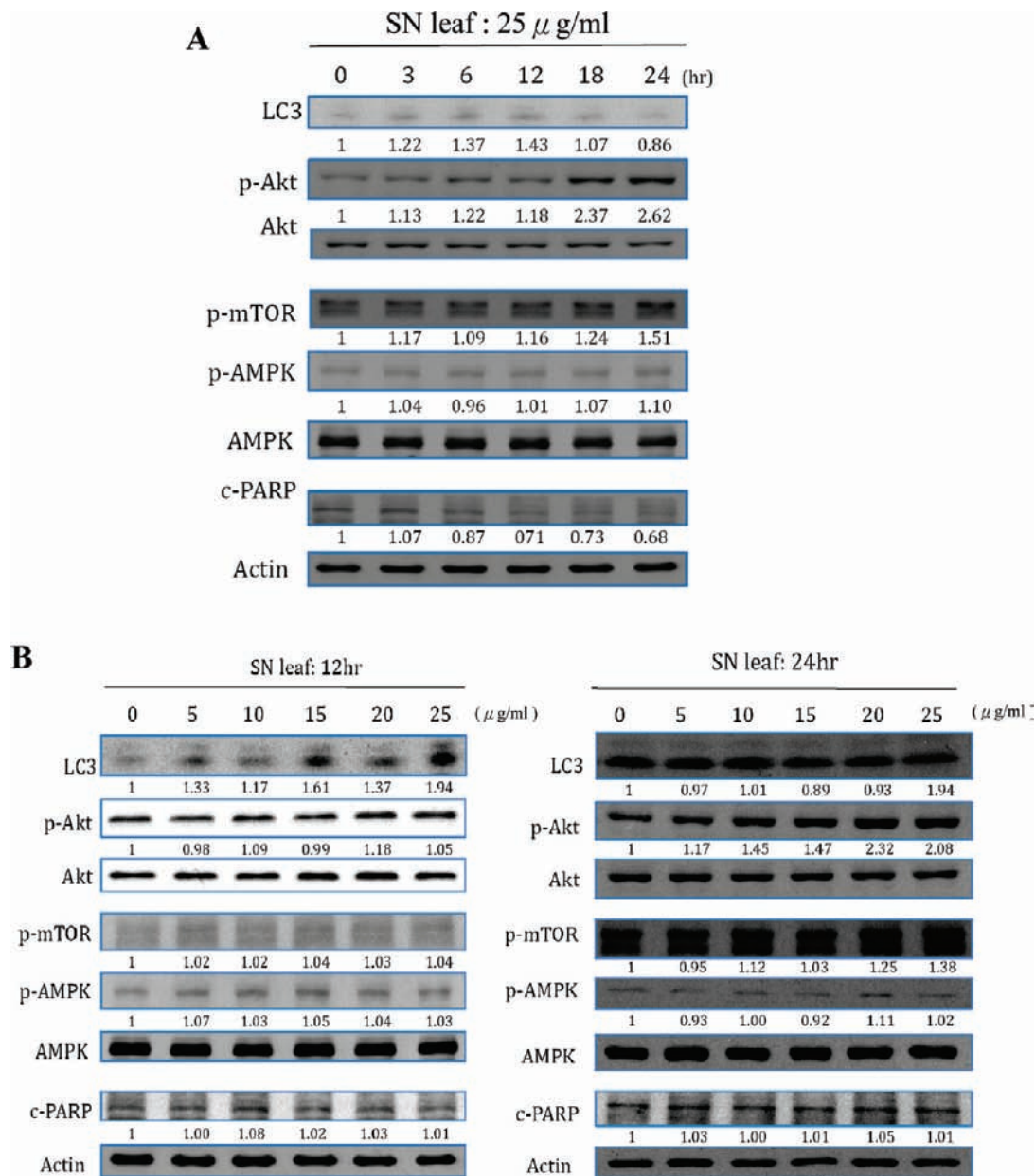


Figure 6. Effects of SN leaf on the LC3, p-AMPK, p-mTOR, p-Akt, and c-PARP in AU565 cells. **(A)** Cells were treated with 25 μ g/mL SN leaf for the indicated times and then subjected to Western blotting. **(B)** Cells were treated with SN leaf at a concentration of 0, 5, 10, 15, 20, or 25 μ g/mL for 12 or 24 h and then subjected to Western blotting. The experiment was performed three times with each antibody, with each yielding similar results. Actin was used as an internal control for equivalent protein loading. The values below the figures represent the change in protein expression of the bands normalized to actin.

may affect mitochondria and then decrease the ATP level in cells. Still other possibilities may contribute to such an effect.

Below 25 μ g/mL SN Leaf Treatment, the Level of LC-3 in AU565 Cells Increased before 12 h, but Decreased after That, Accompanied with the Raising of Phospho-Akt. We next tested the protein level of LC3, the protein marker of autophagy. **Figure 6A** shows that after 25 μ g/mL SN leaf treatment, the LC-3 level increased with a peak at 6–12 h and then decreased after 12 h. The level of p-Akt and p-mTOR (autophagy and apoptosis negative regulator) did not change before 12 h, but increased significantly after 18 h of treatment with SN leaf. **Figure 6B** shows that at 12 h of treatment the LC-3 level increased dose dependently, but other proteins, including p-Akt and p-AMPK, did not change significantly. At 24 h, the LC-3 level did not change after 0–25 μ g/mL SN leaf treatment, and the level of p-Akt and p-mTOR increased dose dependently. Regardless of time or dose test, p-AMPK, an autophagy positive regulator, did not change

significantly. These results suggested the SN leaf induced autophagy in AU565 cells, but the mechanism seemed not related to the down-regulation of p-Akt or the up-regulation of p-AMPK.

A Higher Dose, 100 μ g/mL, of SN Leaf Treatment Induced Cell Death by Autophagy or/and Apoptotic Mechanism. Before, the studies were focused on the dose below 25 μ g/mL that would induce autophagy but not apoptosis. Here is shown the response of AU565 cells after higher doses of SN leaf treatment (50, 100 μ g/mL).

When the concentrations increased from 25 to 100 μ g/mL (for 48 h), the cell viability values of 100 μ g/mL decreased 20% compared to the values of 25 μ g/mL (**Figure 7A**). As shown in **Figure 7B,C**, the cells stop growth (50 μ g/mL) and about 20% are dead (100 μ g/mL) after SN leaf treatment. After 100 μ g/mL SN leaf treatment for 48 h, the protein level of LC-3 and c-PARP was increased, but the level of p-Akt decreased (**Figure 7D**). After 100 μ g/mL SN leaf treat, the cells' morphology (**Figure 4D**) changed; the corpse looked withered and showed more apoptotic

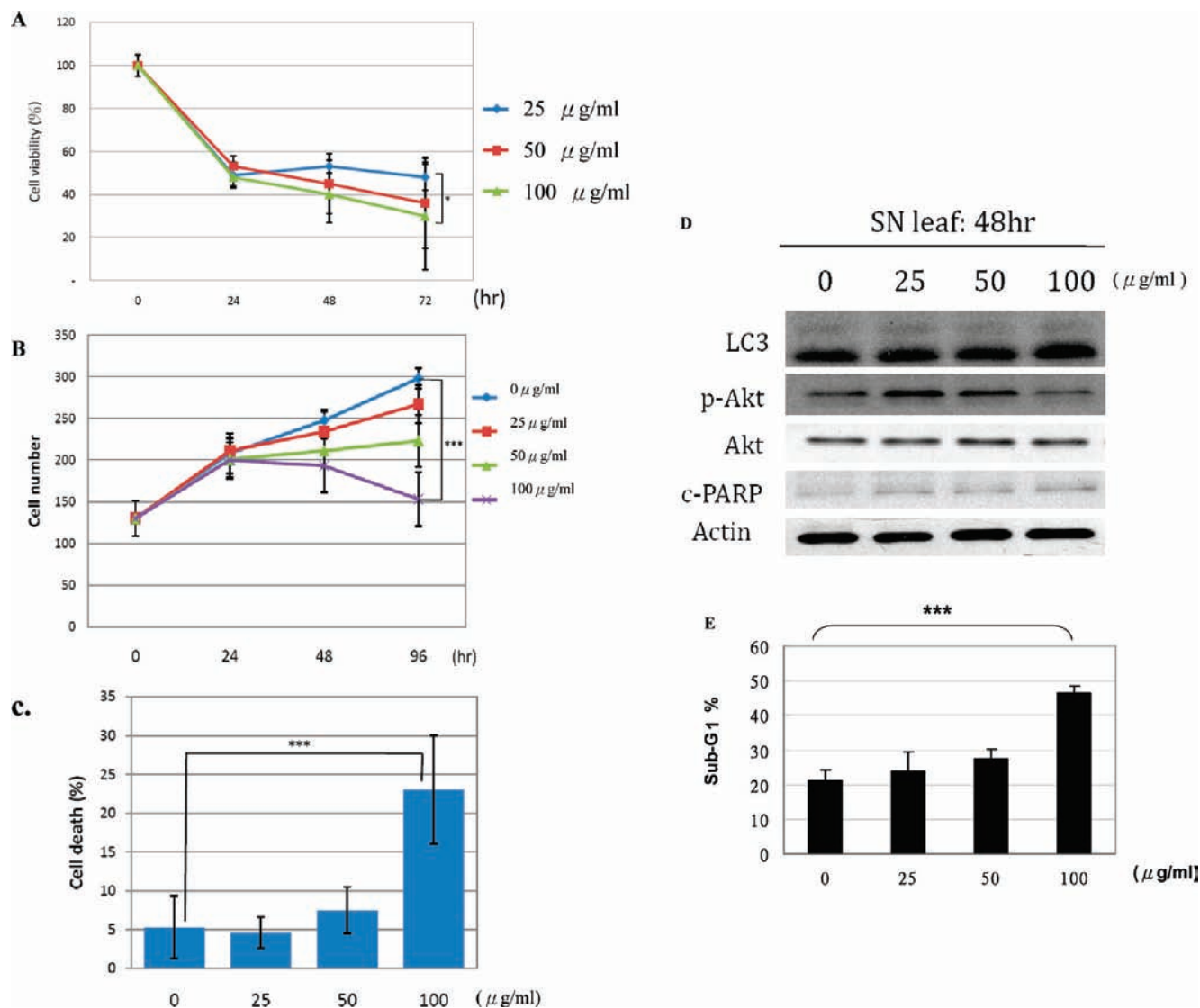


Figure 7. High dose of SN leaf-induced apoptosis and autophagic cell death in AU565 cells. **(A)** Cell growth inhibition was determined by MTT assay. Cells were treated with 50 and 100 $\mu\text{g/ml}$ SN leaf for 24, 48, and 72 h. The number of viable cells after treatment is expressed as a percentage of the vehicle-only control. Data are means of three independent experiments. Bars represent \pm SD. **(B, C)** The cytotoxic effect of SN leaf on AU565 cells was determined using the trypan blue dye exclusion assay, as described under Materials and Methods, and was expressed in terms of the percentage of dead cells as the mean \pm SD of three experiments. **(D)** 100 $\mu\text{g/ml}$ SN leaf treatment may induce not only autophagy but also apoptosis. After 48 h of SN leaf treatment, autophagic marker LC3 and apoptotic marker c-PARP increased slightly at 100 $\mu\text{g/ml}$ accompanied with the decreased of p-Akt. Immunoblotting with β -actin antibody demonstrated an equivalent protein in each lane. **(E)** Cell cycle distribution was assessed by flow cytometry. All values are expressed as mean \pm SD (* indicates the values are significantly different from the control: *, $p < 0.05$; **, $p < 0.01$; ***, $p < 0.001$), $n \geq 3$.

bodies. Moreover, after a treatment with high concentration (100 $\mu\text{g/ml}$) of SN leaf for 48 h, an increased proportion of apoptotic cells was observed (**Figure 7E**). The ratio of cells at the sub-G1 phase was increased to 46.4% when AU565 cells were exposed to 100 $\mu\text{g/ml}$ SN leaf for 48 h, respectively. The results above indicated that long time treatment with 100 $\mu\text{g/ml}$ SN leaf could induce cell death by autophagic and/or apoptotic mechanism.

Effects of Phytochemicals on Cell Viability of AU565 Cells.

The exact autophagy inducer in SN leaf is still unknown. Some known pure compounds that may exist in SN leaf, including coumaric acid, ferulic acid, vanillic acid, cinnamic acid, protocatechuic acid, caffeic acid, syringic acid, chlorogenic acid, gallic acid (**Table 1**), naringenin, rutin, catechin, α -chaconine, solanine, and diosgenin, were chosen to test their effect in AU565 cells (9, 13). Cell viability was decreased by gallic acid, α -chaconine, solanine, and diosgenin (**Figure 8A**). The most abundant polyphenols

in the leaf extracts were gentisic acid, luteolin, apigenin, and kaempferol (**Table 1**). Furthermore, the four phytochemicals were chosen to test their effect in AU565 cells. Cell viability was decreased by four phytochemicals (**Figure 8B**). To determine whether the four phytochemical treatments will induce autophagy, cells were stained with MDC to detect AVO formation. The AVO positive cells increased after luteolin or apigenin treatment (**Figure 8C**). On the basis of these data, we concluded that the SN leaf induced autophagy may not be simply due to one compound effect, and it may be a synergistic effect of more compound cooperation.

DISCUSSION

S. nigrum Linn has been reported to have many anticancer effects, including apoptosis in MCF-7 breast cancer and Hep-G2 liver cancer cells, necrosis in SC-M1 stomach cancer cells, and autophagy in Hep-G2 cells. In our studies, we first compared different parts of SN and identified that SN leaf was more toxic to

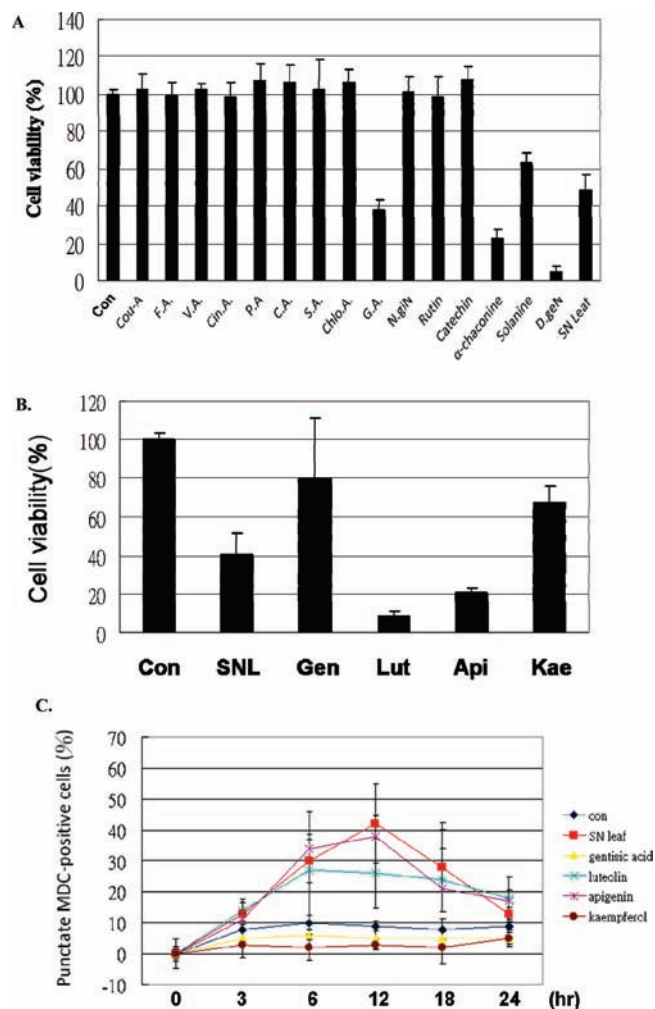


Figure 8. AU565 cells were treated with 25 μ g/mL polyphenols and alkaloids. (A, B) Polyphenols included coumaric acid (cou-A), ferulic acid (F.A.), vanillic acid (V.A.), cinnamic acid (Cin. A.), protocatechuic acid (P.A.), caffeic acid (C.A.), syringic acid (S.A.), chlorogenic acid (Chlo.A.), gallic acid (G.A.), naringenin (N.giN), rutin, catechin luteolin (Lut), apigenin (Api), and kaempferol (Kae). Alkaloids included α -chaconine, solanine, diosgenin (D.geN). Cell growth inhibition was determined by MTT assays. The number of viable cells after treatment is expressed as a percentage of the control. (C) After treatment with SN leaf, gentisic acid, luteolin, apigenin, or kaempferol for different times, cells were stained with MDC. Data are means of three independent experiments. Bars represent the \pm SD.

AU565 breast cancer cells and moderate to NIH-3T3 fibroblasts. Other cell lines such as Hep-G2, MCF-7, and HBL-100 had similar viabilities between AU565 and NIH-3T3 after treatment with SN leaf. These results suggest that SN leaf preferentially inhibited the growth of HER2/*neu*-overexpressing breast cancer cell lines (AU565) but not the cell lines expressing basal levels of HER2/*neu* (MCF-7, HBL-100). These results will provide new information for the study of SN in the future. Numerous studies had demonstrated that polyphenols isolated from many plants exhibit diverse biological activities including immunomodulation and anticancer activities (25, 26). Chow et al. have shown polyphenol patterns in SN; however, the content of the possible bioactive components (polyphenols) in SN was not investigated thoroughly (13). Because we used ethyl acetate extraction for HPLC analysis, the content of polyphenols in our current study might be more than that from the water extraction used in previous studies (13). In this study, we found that SN leaf consists of 11 flavonoids (EGC, EC, EGCG, GCG, rutin, naringenin,

luteolin, quercetin, apigenin, kaempferol, hesperetin) and 8 phenolic acids (gallic acid, protocatechuic acid, gentisic acid, caffeic acid, syringic acid, *p*-coumaric acid, ferulic acid, *m*-coumaric acid) and some unknown polyphenols (Table 1). Apigenin was detected only in SN leaf, not in SN stem and green fruit. The most abundant polyphenols in the leaf extracts were gentisic acid, luteolin, apigenin, kaempferol, and *m*-coumaric acid. The antioxidant and antitumor activities of these extracts have been suggested to be due to the presence of polyphenol constituents. In addition to polyphenol content, we also have studied anthocyanin composition in SNE. However, the anthocyanin existed only in the purple fruits of SN.

Moreover, our results also demonstrated a significant cytotoxic effect of SN leaf on AU565 cells that was mediated via two mechanisms depending on the exposure concentrations. A low dose (< 25 μ g/mL) of SN leaf could induce autophagy but not apoptosis. Higher doses (> 100 μ g/mL) of SN leaf could induce cell death by autophagic and apoptotic mechanisms. However, the molecular basis for the different effects responding to high and low concentrations of SN leaf needs further investigation. There might be cross-talk between the pathways of apoptosis and autophagy.

Nonapoptotic cell death is mainly attributed to autophagy, which is considered to be an alternative way to kill tumor cells when the cells are chemoresistant on the basis of ineffective apoptosis. A number of studies have reported that autophagy is activated in cancer cells in response to various anticancer therapies, such as tamoxifen in breast cancer cells, Temozolomide (TMZ, a DNA alkylating agent), and arsenic trioxide in malignant glioma cells (22). As for natural products, resveratrol, a phytoalexin that is present in grape nuts and red wine, induced autophagy in ovarian cancer cells, and soybean B group triterpenoid saponins caused autophagy in colon cancer cells (13). The results of the present study add SN leaf to the list of natural products that possess autophagic effects in addition to its apoptotic effect.

In AU565 cancer cells, SN leaf-treated cells were able to be stained with acridine orange, a specific marker for autophagic vacuoles (Figure 5A). Confirmatory experiments were performed with anti-LC3 antibody showing that SN leaf stimulated the expression of LC3 protein (Figure 6). Furthermore, we also demonstrated that 3-MA could block SN leaf-induced cell death (Figure 5C). Autophagy responses increased significantly after 6 h of treatment with SN leaf. Autophagy responses gradually decreased after reaching their peak at 18 h (Figure 6). The reasons why the autophagy responses decreased after SN leaf treatment (> 18 h) are not yet clear. It is possible that when excessive autophagy cannot overcome the cell death stimulation, apoptotic cell death does occur and autophagy response decreases (27).

Chow et al. showed that the SN (2 mg/mL) treatment induced the down-regulation of p-Akt and that the SN treatment induced autophagy in Hep-G2 cells (13). Our data did not show the down-regulation of AKT level as a key determinant of autophagy induction by SN leaf (Figure 6). In our studies, 100 μ g/mL SN leaf treatment had similar results as the reduced level of p-Akt accompanied with the increasing level of LC-3 (Figure 7D), but the low dose (25 μ g/mL) of SN leaf treatment increased the p-Akt level (Figure 6A). In previous studies, it has been shown that rapamycin, an inhibitor of mTOR, induces autophagy (28). It is interesting that SN leaf increased AKT phosphorylation, a feature that resembled rapamycin in that rapamycin binds and inhibits mTOR enzymatic activity but through a feedback loop up-regulates AKT expression and activity (29–32). Because SN leaf did not affect mTOR phosphorylation status, whether it directly inhibits mTOR enzymatic activity or interferes with mTOR complex formation with Raptor should be investigated. Therefore,

the molecular mechanisms of a lower dose of SN leaf induced autophagy in AU565 cells deserve further investigation.

In summary, we have identified two distinct antineoplastic activities of SN leaf in breast cancer cells, the abilities to induce apoptosis and autophagocytosis. The results support further investigation of its merit as a potential drug candidate for therapy of caspase-resistant recurrent breast cancer, either as a single modality or in combination with other drugs.

LITERATURE CITED

- Zakaria, Z. A.; Gopalan, H. K.; Zainal, H.; Mohd Pojan, N. H.; Morsid, N. A.; Aris, A.; Sulaiman, M. R. Antinociceptive, anti-inflammatory and antipyretic effects of *Solanum nigrum* chloroform extract in animal models. *Yakugaku Zasshi* **2006**, *126*, 1171–1178.
- Dafni, A.; Yaniv, Z. Solanaceae as medicinal plants in Israel. *J. Ethnopharmacol.* **1994**, *44*, 11–18.
- Lin, H. M.; Tseng, H. C.; Wang, C. J.; Lin, J. J.; Lo, C. W.; Chou, F. P. Hepatoprotective effects of *Solanum nigrum* Linn extract against CCl₄-induced oxidative damage in rats. *Chem.–Biol. Interact.* **2008**, *171*, 283–293.
- An, L.; Tang, J. T.; Liu, X. M.; Gao, N. N. [Review about mechanisms of anti-cancer of *Solanum nigrum*]. *Zhongguo Zhong Yao Za Zhi* **2006**, *31*, 1225–1226, 1260.
- Sultana, S.; Perwaiz, S.; Iqbal, M.; Athar, M. Crude extracts of hepatoprotective plants, *Solanum nigrum* and *Cichorium intybus* inhibit free radical-mediated DNA damage. *J. Ethnopharmacol.* **1995**, *45*, 189–192.
- Prashanth Kumar, V.; Shashidhara, S.; Kumar, M. M.; Sridhara, B. Y. Cytoprotective role of *Solanum nigrum* against gentamicin-induced kidney cell (Vero cells) damage in vitro. *Fitoterapia* **2001**, *72*, 481–486.
- Akhtar, M. S.; Munir, M. Evaluation of the gastric antiulcerogenic effects of *Solanum nigrum*, *Brassica oleracea* and *Ocimum basilicum* in rats. *J. Ethnopharmacol.* **1989**, *27*, 163–176.
- Heo, K. S.; Lim, K. T. Glycoprotein isolated from *Solanum nigrum* L. modulates the apoptotic-related signals in 12-*O*-tetradecanoylphorbol 13-acetate-stimulated MCF-7 cells. *J. Med. Food* **2005**, *8*, 69–77.
- Son, Y. O.; Kim, J.; Lim, J. C.; Chung, Y.; Chung, G. H.; Lee, J. C. Ripe fruit of *Solanum nigrum* L. inhibits cell growth and induces apoptosis in MCF-7 cells. *Food Chem. Toxicol.* **2003**, *41*, 1421–1428.
- Hsu, J. D.; Kao, S. H.; Tu, C. C.; Li, Y. J.; Wang, C. J. *Solanum nigrum* L. extract inhibits 2-acetylaminofluorene-induced hepatocarcinogenesis through overexpression of glutathione *S*-transferase and antioxidant enzymes. *J. Agric. Food Chem.* **2009**, *57*, 8628–8634.
- Ikedo, T.; Tsumagari, H.; Nohara, T. Steroidal oligoglycosides from *Solanum nigrum*. *Chem. Pharm. Bull. (Tokyo)* **2000**, *48*, 1062–1064.
- Li, J.; Li, Q. W.; Gao, D. W.; Han, Z. S.; Li, K. Antitumor effects of total alkaloids isolated from *Solanum nigrum* in vitro and in vivo. *Pharmazie* **2008**, *63*, 534–538.
- Lin, H. M.; Tseng, H. C.; Wang, C. J.; Chyau, C. C.; Liao, K. K.; Peng, P. L.; Chou, F. P. Induction of autophagy and apoptosis by the extract of *Solanum nigrum* Linn in HepG2 cells. *J. Agric. Food Chem.* **2007**, *55*, 3620–3628.
- Joo, H. Y.; Lim, K.; Lim, K. T. Phytoglycoprotein (150 kDa) isolated from *Solanum nigrum* Linne has a preventive effect on dextran sodium sulfate-induced colitis in A/J mouse. *J. Appl. Toxicol.* **2009**, *29*, 207–213.
- Yang, Y. P.; Liang, Z. Q.; Gu, Z. L.; Qin, Z. H. Molecular mechanism and regulation of autophagy. *Acta Pharmacol. Sin.* **2005**, *26*, 1421–1434.
- Heymann, D. Autophagy: a protective mechanism in response to stress and inflammation. *Curr. Opin. Invest. Drugs* **2006**, *7*, 443–450.
- Marino, G.; Lopez-Otin, C. Autophagy: molecular mechanisms, physiological functions and relevance in human pathology. *Cell. Mol. Life Sci.* **2004**, *61*, 1439–1454.
- Deretic, V. Autophagy as an immune defense mechanism. *Curr. Opin. Immunol.* **2006**, *18*, 375–382.
- Bursch, W.; Ellinger, A. Autophagy – a basic mechanism and a potential role for neurodegeneration. *Folia Neuropathol.* **2005**, *43*, 297–310.
- Yang, Y. P.; Liang, Z. Q.; Gao, B.; Jia, Y. L.; Qin, Z. H. Dynamic effects of autophagy on arsenic trioxide-induced death of human leukemia cell line HL60 cells. *Acta Pharmacol. Sin.* **2008**, *29*, 123–134.
- Harada, M.; Hanada, S.; Toivola, D. M.; Ghori, N.; Omary, M. B. Autophagy activation by rapamycin eliminates mouse Mallory–Denk bodies and blocks their proteasome inhibitor-mediated formation. *Hepatology* **2008**, *47*, 2026–2035.
- de Medina, P.; Silvente-Poirot, S.; Poirot, M. Tamoxifen and AEBs ligands induced apoptosis and autophagy in breast cancer cells through the stimulation of sterol accumulation. *Autophagy* **2009**, *5*, 1066–1067.
- Lin, C. M.; Chen, C. S.; Chen, C. T.; Liang, Y. C.; Lin, J. K. Molecular modeling of flavonoids that inhibits xanthine oxidase. *Biochem. Biophys. Res. Commun.* **2002**, *294*, 167–172.
- Plomp, P. J.; Gordon, P. B.; Meijer, A. J.; Hoyvik, H.; Seglen, P. O. Energy dependence of different steps in the autophagic-lysosomal pathway. *J. Biol. Chem.* **1989**, *264*, 6699–6704.
- Fiuza, S. M.; Gomes, C.; Teixeira, L. J.; Girao da Cruz, M. T.; Cordeiro, M. N.; Milhazes, N.; Borges, F.; Marques, M. P. Phenolic acid derivatives with potential anticancer properties – a structure–activity relationship study. Part 1: methyl, propyl and octyl esters of caffeic and gallic acids. *Bioorg. Med. Chem.* **2004**, *12*, 3581–3589.
- Gomes, C. A.; da Cruz, T. G.; Andrade, J. L.; Milhazes, N.; Borges, F.; Marques, M. P. Anticancer activity of phenolic acids of natural or synthetic origin: a structure–activity study. *J. Med. Chem.* **2003**, *46*, 5395–5401.
- Hsu, K. F.; Wu, C. L.; Huang, S. C.; Wu, C. M.; Hsiao, J. R.; Yo, Y. T.; Chen, Y. H.; Shiau, A. L.; Chou, C. Y. Cathepsin L mediates resveratrol-induced autophagy and apoptotic cell death in cervical cancer cells. *Autophagy* **2009**, *5*, 451–460.
- Ravikumar, B.; Vacher, C.; Berger, Z.; Davies, J. E.; Luo, S.; Oroz, L. G.; Scaravilli, F.; Easton, D. F.; Duden, R.; O’Kane, C. J.; Rubinsztein, D. C. Inhibition of mTOR induces autophagy and reduces toxicity of polyglutamine expansions in fly and mouse models of Huntington disease. *Nat. Genet.* **2004**, *36*, 585–595.
- Wan, X.; Harkavy, B.; Shen, N.; Grohar, P.; Helman, L. J. Rapamycin induces feedback activation of Akt signaling through an IGF-1R-dependent mechanism. *Oncogene* **2007**, *26*, 1932–1940.
- O’Reilly, K. E.; Rojo, F.; She, Q. B.; Solit, D.; Mills, G. B.; Smith, D.; Lane, H.; Hofmann, F.; Hicklin, D. J.; Ludwig, D. L.; Baselga, J.; Rosen, N. mTOR inhibition induces upstream receptor tyrosine kinase signaling and activates Akt. *Cancer Res.* **2006**, *66*, 1500–1508.
- Sun, S. Y.; Rosenberg, L. M.; Wang, X.; Zhou, Z.; Yue, P.; Fu, H.; Khuri, F. R. Activation of Akt and eIF4E survival pathways by rapamycin-mediated mammalian target of rapamycin inhibition. *Cancer Res.* **2005**, *65*, 7052–7058.
- Hu, H.; Chai, Y.; Wang, L.; Zhang, J.; Lee, H. J.; Kim, S. H.; Lu, J. Pentagalloylglucose induces autophagy and caspase-independent programmed deaths in human PC-3 and mouse TRAMP-C2 prostate cancer cells. *Mol. Cancer Ther.* **2009**, *8*, 2833–2843.

Received for review March 16, 2010. Revised manuscript received May 25, 2010. Accepted May 26, 2010. This study was supported by National Science Council NSC 96-2321-B-002-026 and NSC 97-2321-B-002-016.